Selectivity in coherent transient Raman measurements of vibrational dephasing in liquids

Roger F. Loring and Shaul Mukamel[a)]
Department of Chemistry, University of Rochester, Rochester, New York 14627

(Received 4 February 1985; accepted 30 May 1985)

The microscopic information content of coherent transient Raman measurements is analyzed. It is shown that for short pulses and optically thin samples the Kaiser–Laubereau pulse sequence is the Raman analog of the optical free induction decay, and that the experimental observable contains the same dynamical information as the isotropic, spontaneous Raman line shape. Under these conditions, the experiment therefore cannot be used to selectively measure the homogeneous dephasing time of a system with an inhomogeneously broadened line. The results of our analysis are at variance with the earlier results of Kaiser and Laubereau and the more recent predictions of Oxtoby. However, these experiments, under certain circumstances, may be used to obtain a nonselective line narrowing, as found by Zinth, Polland, Laubereau, and Kaiser. We also consider the situation in which the sample is optically dense, in which case laser depletion must be taken into account. The distinction between saturation of the vibrational transition and depletion of the pump pulse is discussed, and selectivity is shown to arise from the former phenomenon, rather than from the latter. This result is at variance with the predictions of George and Harris. An alternative pulse sequence, the Raman echo, is suggested as a tool to achieve selectivity. A unified theory of the Raman echo is developed, which is valid for a bath with arbitrary time scale and which interpolates between the limits of homogeneous and inhomogeneous line broadening.

I. INTRODUCTION

In the last decade, considerable attention has been given to the study of the dynamics of vibrational excitations in liquids.[1–6] Before the advent of picosecond spectroscopic methods, vibrational dephasing in liquids was studied through measurements of the isotropic Raman line shape, $\hat{I}_0(\omega)$.[2–6] This line shape is proportional to the Fourier transform of the vibrational correlation function $\langle \hat{q}(t)\hat{q}(0)\rangle$, where $\hat{q}$ is the coordinate of the relevant vibrational mode, and the angular brackets indicate a trace over the equilibrium density matrix[7]:

$$I_0(t) = \langle \hat{q}(t)\hat{q}(0)\rangle, \tag{1.1}$$

$$\hat{I}_0(\omega) = \int_{-\infty}^{\infty} dt \exp[i\omega t]\, I_0(t). \tag{1.2}$$

The distinction is traditionally made between homogeneous and inhomogeneous contributions to spectral line shapes. When different molecules absorb at different frequencies because of different local environments or different initial states, the line is said to be inhomogeneously broadened. This broadening is *static* in nature, reflecting the spread in molecular transition frequencies, and carries no dynamical information. It may be shown using the central limit theorem that when the interaction with the environment is the sum of many small contributions, the resulting line shape assumes a Gaussian form. However, in general the inhomogeneously broadened line can assume any form and is not necessarily a Gaussian. Homogeneous broadening arises from an interaction with a bath with a very fast time scale, such as rapid fluctuations in the local environment. As far as the radiation field is concerned, all molecules on the average appear identical. The resulting line shape for a two-level system is a Lorentzian corresponding to an exponential decay of the correlation function $I_0(t)$. Although these two limits are well defined, the classification of realistic line broadening mechanisms into these two categories is not always possible. Consider a molecule coupled to a bath with time scale τ_c. If τ_c^{-1} is much smaller than the observed linewidth, the line is inhomogeneously broadened. As τ_c^{-1} is increased, the line shape will change, and only when τ_c^{-1} is much larger than the observed linewidth, will a Lorentzian, homogeneously broadened line emerge. For intermediate τ_c^{-1}, the line cannot be classified as either homogeneously or inhomogeneously broadened. Stochastic[7] and microscopic[6,8] models which are valid for arbitrary τ_c and interpolate between these limits, allow a more realistic calculation of spectral line shapes in liquids.

A major problem in the interpretation of ordinary line shapes, such as $\hat{I}_0(\omega)$, is that the same line shape may arise from homogeneous, inhomogeneous, or intermediate mechanisms. It is, therefore, impossible to extract dynamical information from the line shape alone without more detailed information from another source. Moreover, in many cases several broadening mechanisms coexist. Often, the inhomogeneous contribution is sufficiently large that the dynamical (homogeneous) information is hidden under the inhomogeneously broadened envelope. This situation is common in the study of electronic dephasing in molecular solids. In such systems, the absorption line shape is inhomogeneously broadened from crystal strains and defects, and this inhomogeneous broadening obscures the broadening due to intrinsic molecular processes.[9] Sophisticated techniques, such as hole burning,[10] fluorescence line narrowing,[11] and photon ech-

[a)] Camille and Henry Dreyfus Teacher–Scholar.

 0021-9606/85/172116-13$02.10

oes[12] can be used to eliminate (partially or entirely) the inhomogeneous broadening and to extract dynamical information, even in cases in which the line shape is dominated by inhomogeneous contributions. Multiple pulse sequences in NMR[13(a)] and their optical analogs[13(b)] provide a beautiful example of a selective elimination of unwanted information.

Sophisticated techniques have likewise been developed to study the dephasing of vibrations in liquids. In these experiments, an initial simultaneous pair of picosecond pulses prepares a coherent superposition of two vibrational states by stimulated Raman scattering. After a delay period, another pulse probes the coherence through a coherent Raman process. Kaiser, Laubereau and co-workers,[1,14] and Harris and co-workers[3] have used this technique to measure vibrational dephasing times in several liquids. This technique has also been applied to the study of vibrational relaxation in molecular crystals by Hochstrasser *et al.*,[15(a)] Wiersma *et al.*,[15(b)] and Dlott *et al.*[15(c)] For certain liquids the measured dephasing times correspond to a linewidth that is narrower than the isotropic Raman linewidth. The early theoretical treatments of this problem by Laubereau *et al.*[1,14(a)] and the theory of Oxtoby[5] lead to the prediction that the spatial phase matching condition in these experiments makes them *selective*. Selectivity was defined in this context for a particular model system. In this model, the liquid is composed of M molecular species, and each species is taken to have a homogeneously broadened line. The isotropic Raman line shape is given by

$$\hat{I}_0(\omega) = \sum_{j=1}^{M} N_j \hat{I}_0^{(j)}(\omega)$$

$$= \sum_{j=1}^{M} N_j (\Gamma_j/\pi)[(\omega-\omega_j)^2+\Gamma_j^2]^{-1}. \qquad (1.3)$$

N_j is the relative concentration of the jth species, and $\hat{I}_0^{(j)}(\omega)$ is its line shape. In this model, a homogeneous source and an inhomogeneous source of line broadening coexist. Selectivity was defined as the capacity of the coherent experiment to selectively measure the dephasing time $T_2 = \Gamma_j^{-1}$ of a particular species, even when $\hat{I}_0^{(j)}(\omega)$ overlaps with other lines. These theoretical analyses[1,5,14(a)] thus led to the conclusion that the coherent transient Raman experiments are capable of measuring homogeneous dephasing times in systems with static, inhomogeneous broadening.

It was later determined by Kaiser and co-workers[14(b)] that their measured dephasing times were correlated with the durations of the excitation laser pulses, and that under their experimental conditions the experiment is not selective. They concluded that, although the technique results in line narrowing, the measured linewidths are instrumental and do not contain any dynamical information. However, it is not clear from their analysis if the absence of selectivity is intrinsic to the technique, in which case an explicit error must be found in the previous analyses[5,14(a)] or that the conditions for selectivity were simply not met in those particular experiments. George and Harris[16] have carried out a calculation of the experimental observable for the situation in which the initial laser pump pulse is significantly depleted by an optically dense sample. They argued that for sufficiently high laser depletion it is possible to extract a homogeneous dephasing time from a system with static inhomogeneous broadening, even when this may not be the case for low laser depletion. Thus, there exists considerable controversy in the literature concerning the nature of the microscopic quantity that is being measured in these experiments.

In this work, we investigate the coherent transient vibrational dephasing experiment and analyze its information content. We shall address the issue of selectivity in a broader sense by asking the following question, which is not restricted to the particular form of $\hat{I}_0(\omega)$ [Eq. (1.3)]: does the coherent transient Raman observable contain more information than $\hat{I}_0(\omega)$ by virtue of the phase-matching condition? We show that for optically thin samples and short pulses the answer to this question is negative. The experiment is, under these conditions, not selective in principle. This finding is in disagreement with the earlier conclusions of Laubereau *et al.*[14(a)] and Oxtoby.[5] Unlike the previous treatments,[1,5,14(a)] our theory is based on a correlation function approach which treats the entire process as one event without separating it into preparation, propagation, and detection stages. Since the information content of this experiment is the same as that of an optical free induction decay experiment, we denote it the Raman free induction decay (RFID). We also consider circumstances under which the experimental observable can contain more information than the low power line shape, $\hat{I}_0(\omega)$. If the laser pulses are long and sufficiently strong to saturate the vibrational transition, the RFID observable will no longer depend only on the low power line shape. The calculation of George and Harris allows for the depletion of the pump laser pulse, but it does not include saturation of the vibrational transition. We demonstrate that under these assumptions the information content of the experiment is still equivalent to that of $\hat{I}_0(\omega)$. The distinction between pulse depletion and material saturation is crucial. For example, a long, strong pulse, acting on an optically thin sample, may saturate the transition without being appreciably depleted. It is saturation of the transition, rather than pulse depletion, that can lead to selectivity in this experiment. This finding is at variance with the conclusions of George and Harris. The nature of the observable for the case of long, strong pulses is more complex and requires further analysis.

We propose that vibrational dephasing in liquids be studied with a different experiment, the Raman echo (RE), which is the analog of the optical photon echo[12] and is capable of providing dynamical information that cannot be obtained from $\hat{I}_0(\omega)$. The RE was originally proposed by Hartmann[17] and has been carried out in gas phase[18] and solid state[19] systems. If the broadening of vibrational lines in liquids can be described as a combination of a static inhomogeneous contribution and a dynamic homogeneous contribution [Eq. (1.3)], the homogeneous dephasing time can be unambiguously determined with the RE. We present a unified theory of the RE that is valid for a bath with arbitrary time scale and interpolates between the limiting cases of homogeneous and inhomogeneous broadening.

In Sec. II we present the model system and discuss the calculation of the RFID and RE observables. Section III contains the results of these calculations. It is demonstrated that for short pulses and optically thin samples, the RFID is

incapable of providing dynamical information that goes beyond the information content of the isotropic Raman line shape $\hat{I}_0(\omega)$. Such selectivity can be obtained, however, with the RE. In Sec. IV we analyze the treatments of Laubereau *et al.*[14(a)] and Oxtoby[5] for optically thin samples, which lead to the opposite conclusion, namely that the RFID experiment can be selective. We show that the phase matching condition was incorrectly introduced in these studies. In Sec. V, we discuss the high laser depletion limit of George and Harris.[16] Section VI summarizes our results.

II. MODEL AND OBSERVABLES

We model the molecular liquid as a collection of three-level systems of the type depicted in Fig. 1. $|1\rangle$ and $|2\rangle$ denote vibronic states belonging to the manifold of the ground electronic state, whereas the vibronic state $|3\rangle$ belongs to an electronically excited state. States $|1\rangle$ and $|3\rangle$ and states $|2\rangle$ and $|3\rangle$ are connected by transition dipoles μ_{13} and μ_{23}, respectively. The energy difference between $|3\rangle$ and $|1\rangle$ is $\hbar\Omega_3$, and the energy difference between $|2\rangle$ and $|1\rangle$ is $\hbar\Omega_2 + \hbar\Delta(t)$. $\Delta(t)$ is a stochastic process with zero mean arising from the random force exerted on the absorber molecule by its fluctuating environment. The effect of this fluctuating energy is to broaden the spontaneous Raman line shape for the $|1\rangle$ to $|2\rangle$ transition (proper dephasing).[7,8]

The Raman free induction decay (RFID) and the Raman echo (RE) experiments both begin with a pair of time-coincident pulses that excite a coherence between $|1\rangle$ and $|2\rangle$ by stimulated Stokes scattering. This electric field is given by

$$E(z,t) = E_L(z,t)\cos(\omega_L t - k_L z) + E_S(z,t)\cos(\omega_S t - k_S z), \tag{2.1}$$

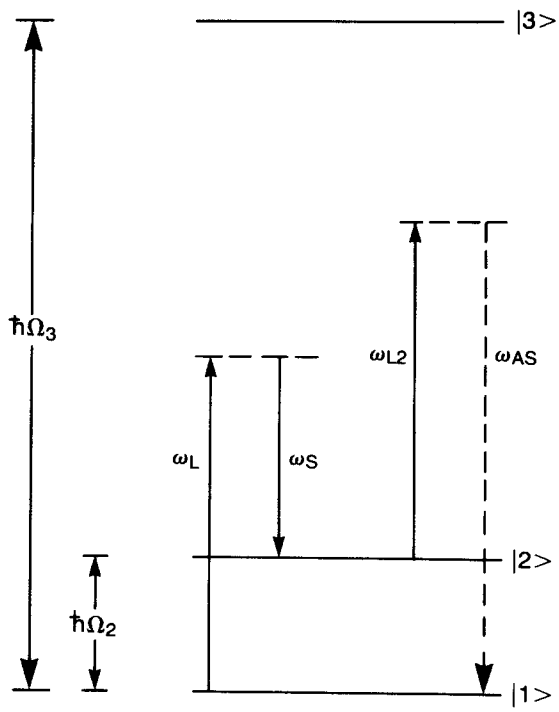

FIG. 1. Energy level diagram for the model system discussed in Sec. II.

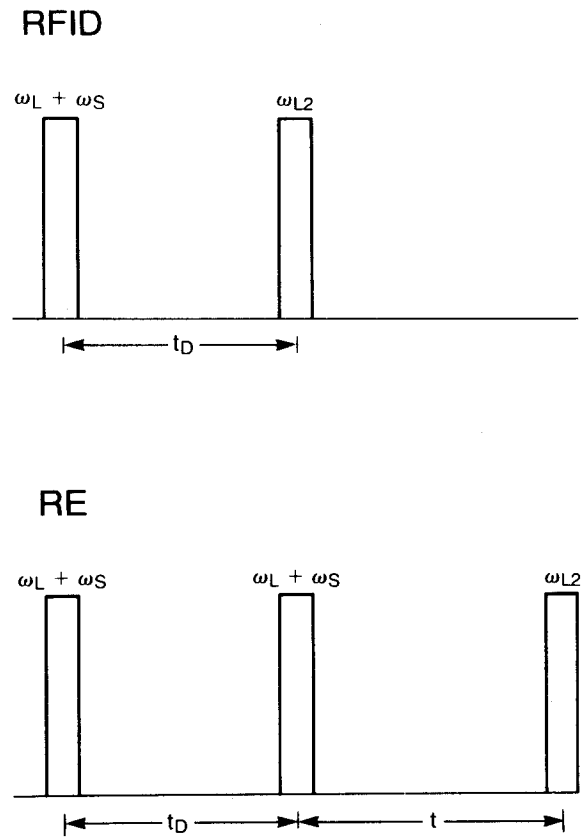

FIG. 2. Pulse sequences for Raman free induction decay and Raman echo experiments.

where $\omega_L = \Omega_2 + \omega_S$, as shown in Fig. 1. There follows a delay period of duration t_D. In the RFID, the system is then irradiated by a probe pulse

$$E(z,t) = E_{L2}(z,t)\cos(\omega_{L2} t - k_{L2} z) \tag{2.2}$$

and emission is detected at frequency $\omega_{L2} - \Omega_2$ (Stokes) or frequency $\omega_{L2} + \Omega_2$ (anti-Stokes). In the RE, the system is irradiated with another pair of excitation pulses of the form given in Eq. (2.1). After another delay period of duration t, the system is probed with a pulse of the form given in Eq. (2.2), and the coherent Stokes or anti-Stokes signal is detected. The RFID consists of one pair of excitation pulses, one delay period, and a probe pulse, while the RE consists of two pairs of excitation pulses, two delay periods, and a probe pulse. The pulse sequences are shown in Fig. 2. For each experiment we will calculate the signal as follows. We first calculate the three-level system density matrix ρ after a given pulse sequence, using the Liouville equation,

$$d\rho/dt = (-i/\hbar)[H,\rho], \tag{2.3}$$

where H is the relevant Hamiltonian. The absorbers are assumed not to interact, so the density matrix of the entire system factors into a product of molecular density matrices and the calculation can be carried out using ρ for a single three-level system. The ensemble averaged polarization per molecule P can then be calculated from

$$P = \langle \mathrm{Tr}\,\mu\rho \rangle, \tag{2.4}$$

where μ is the transition dipole operator, and the brackets denote the ensemble average over the stochastic variable

$\Delta(t)$. P can then be used as a source in Maxwell's equations to calculate the intensity of the signal.

The evolution of the density matrix, in the absence of an electromagnetic field, is given by

$$\rho(t) = U(t,0)\rho(0)U^{\dagger}(t,0), \tag{2.5a}$$

$$U(t,0) = \exp_{+}\left[\frac{-i}{\hbar}\int_0^t d\tau\, H_0(\tau)\right], \tag{2.5b}$$

$$H_0(\tau) = \hbar[\Omega_2 + \Delta(\tau)]|2\rangle\langle 2| + \hbar\Omega_3|3\rangle\langle 3|. \tag{2.5c}$$

In Eq. (2.5b), $\exp_+$ is the usual time-ordered exponential.[20]

We next consider the evolution of the density matrix during a pulse of the form given in Eq. (2.1). The following simplifying assumptions are made. All transition dipoles are parallel to the electric field vectors. The temporal profile of each pulse is rectangular. The pulses are sufficiently short that the fluctuation in the energy of $|2\rangle$ can be neglected during the pulse. The excitations are sufficiently far off resonance that we need only consider the coupling of E_L to μ_{13} and the coupling of E_S to μ_{23}. This last assumption is discussed by Hartmann.[17] Within these assumptions, the Hamiltonian during the pulse is given by

$$\begin{aligned} H(t) = &-\mu_{13}E_L\cos(\omega_L t - k_L z)[|1\rangle\langle 3| + |3\rangle\langle 1|] \\ &-\mu_{23}E_S\cos(\omega_S t - k_S z)[|2\rangle\langle 3| + |3\rangle\langle 2|] \\ &+\hbar\Omega_2|2\rangle\langle 2| + \hbar\Omega_3|3\rangle\langle 3|. \end{aligned} \tag{2.6}$$

We make the transformation[17]

$$\tilde{\rho}(t) = S^{\dagger}(t)\rho(t)S(t), \tag{2.7}$$

where

$$S(t) = |1\rangle\langle 1|\exp(i\omega_L t) + |2\rangle\langle 2|\exp(i\omega_S t) + |3\rangle\langle 3|. \tag{2.8}$$

Substituting Eq. (2.7) into Eq. (2.3) and making the rotating wave approximation[17] yields

$$d\tilde{\rho}/dt = -i[H', \tilde{\rho}], \tag{2.9}$$

where

$$\begin{aligned} H' = &\omega_L|1\rangle\langle 1| \\ &+(\Omega_2 + \omega_S)|2\rangle\langle 2| + \Omega_3|3\rangle\langle 3| - \Omega_{13}|1\rangle\langle 3| \\ &-\Omega_{13}^{*}|3\rangle\langle 1| - \Omega_{23}|2\rangle\langle 3| - \Omega_{23}^{*}|3\rangle\langle 2|, \end{aligned} \tag{2.10a}$$

$$\Omega_{13} = (\mu_{13}E_L/2\hbar)\exp(-ik_L z), \tag{2.10b}$$

$$\Omega_{23} = (\mu_{23}E_S/2\hbar)\exp(-ik_S z). \tag{2.10c}$$

The density matrix after a pair of excitation pulses of duration τ is given by

$$\rho(t+\tau) = S(\tau)V(\tau)\rho(t)V^{\dagger}(\tau)S^{\dagger}(\tau), \tag{2.11a}$$

$$V(\tau) = \exp[-iH'\tau]. \tag{2.11b}$$

The matrix elements of $V(\tau)$ can be determined in a straightforward manner by carrying out the Laplace transform of Eq. (2.11b) to give

$$\hat{V}(s) = [s + iH']^{-1}, \tag{2.12}$$

where s is the Laplace variable. The matrix $s + iH'$ is easily inverted, and inverse Laplace transformation of the elements of $\hat{V}(s)$ yields $V(\tau)$. We will need $V_{11}(\tau)$, $V_{12}(\tau)$, and $V_{21}(\tau)$, which are given by

$$V_{11}(\tau) = \exp(-i\omega_L\tau)[|\Omega_{13}|^2\exp(i\omega\tau) + |\Omega_{23}|^2]\gamma^{-2} \tag{2.13a}$$

$$V_{12}(\tau) = -\Omega_{13}\Omega_{23}^{*}\exp(-i\omega_L\tau)[1 - \exp(i\omega\tau)]\gamma^{-2}, \tag{2.13b}$$

$$V_{21}(\tau) = [V_{12}(-\tau)]^{*}, \tag{2.13c}$$

$$\gamma^2 = |\Omega_{13}|^2 + |\Omega_{23}|^2, \tag{2.13d}$$

$$\omega = \gamma^2/(\Omega_3 - \omega_L). \tag{2.13e}$$

These results are valid in the limit

$$4\gamma^2 \ll (\Omega_3 - \omega_L)^2. \tag{2.14}$$

This condition will be satisfied if the excitation pulse is sufficiently nonresonant.[17]

We next consider the evolution of the density matrix during the probe pulse of Eq. (2.2). For simplicity we will calculate only the anti-Stokes signal for both RFID and RE experiments. Therefore, we will only consider the coupling of the probe pulse to μ_{23} and neglect the coupling to μ_{13} which will produce the Stokes signal. The Hamiltonian during the probe pulse is given by

$$\begin{aligned} H_p/\hbar = &\Omega_2|2\rangle\langle 2| + \Omega_3|3\rangle\langle 3| - (\mu_{23}E_{L2}/\hbar)\cos(\omega_{L2}t - k_{L2}z) \\ &\times[|2\rangle\langle 3| + |3\rangle\langle 2|]. \end{aligned} \tag{2.15}$$

This Hamiltonian has the same form as the Hamiltonian of Eq. (2.6) in the absence of the field that couples to μ_{13}. Thus, the methods just described can be used to solve for the time evolution of the density matrix during the probe pulse. The density matrix after a probe pulse of duration τ is given by

$$\rho(t+\tau) = S_p(\tau)V_p(\tau)\rho(t)V_p^{\dagger}(\tau)S_p^{\dagger}(\tau), \tag{2.16}$$

where $S_p(\tau)$ is the rotating frame transformation

$$S_p(\tau) = (|1\rangle\langle 1| + |2\rangle\langle 2|)\exp(i\omega_{L2}t) + |3\rangle\langle 3|. \tag{2.17}$$

The propagator $V_p(\tau)$ is given by

$$V_p(\tau) = \exp[-iH_p'\tau], \tag{2.18a}$$

$$\begin{aligned} H_p' = &\omega_{L2}|1\rangle\langle 1| + \omega_{AS}|2\rangle\langle 2| \\ &+\Omega_3|3\rangle\langle 3| - \Omega_p|2\rangle\langle 3| \\ &-\Omega_p^{*}|3\rangle\langle 2|, \end{aligned} \tag{2.18b}$$

$$\omega_{AS} = \Omega_2 + \omega_{L2}, \tag{2.18c}$$

$$\Omega_p = (\mu_{23}E_{L2}/2\hbar)\exp(-ik_{L2}z). \tag{2.18d}$$

We will need elements $[V_p(\tau)]_{11}$ and $[V_p(\tau)]_{23}$ in the calculation. These elements can be evaluated with the method discussed following Eq. (2.11b):

$$[V_p(\tau)]_{11} = \exp(-i\omega_{L2}\tau), \tag{2.19a}$$

$$\begin{aligned} [V_p(\tau)]_{23} = &\frac{\Omega_p(\Omega_3 - \omega_{AS})}{(\Omega_3 - \omega_{AS})^2 + 2|\Omega_p|^2}\{\exp(i\Omega_3\tau) \\ &-\exp[i\omega_{AS}\tau]\}, \end{aligned} \tag{2.19b}$$

$$[V_p(\tau)]_{32} = [V_p(-\tau)]_{23}^{*}. \tag{2.19c}$$

Equation (2.19b) is an approximation that is valid for a condition similar to that of Eq. (2.14):

$$4|\Omega_p|^2 \ll (\Omega_3 - \omega_{AS})^2. \tag{2.20}$$

Equation (2.20) will be satisfied if the probe pulse is sufficiently nonresonant.

In the RFID experiment, the sample is excited for a time τ_1, is allowed to evolve freely for a time t_D, and then is probed for a time τ_p. The density matrix directly after the probe pulse is given by

$$\rho(\tau_1 + t_D + \tau_p) = S_p(\tau_p)V_p(\tau_p)U(t_D, 0)S(\tau_1)V(\tau_1)\rho(0)V^\dagger(\tau_1) \times S^\dagger(\tau_1)U^\dagger(t_D, 0)\, V_p^\dagger(\tau_p)S_p^\dagger(\tau_p). \quad (2.21)$$

The macroscopic polarization that produces the coherent anti-Stokes signal can be calculated from $\rho_{13}(\tau_1 + t_D + \tau_p)$. This matrix element is the sum of a term proportional to $\rho_{12}(\tau_1 + t_D)$ and a term proportional to $\rho_{13}(\tau_1 + t_D)$. For the case of nonresonant excitation [see Eq. (2.14)], the coherence induced between $|1\rangle$ and $|3\rangle$ by the initial excitation pulses can be neglected. In this case, $\rho_{13}(\tau_1 + t_D + \tau_p)$ is given by

$$\rho_{13}(\tau_1 + t_D + \tau_p) = [S_p(\tau_p)]_{11}[V_p(\tau_p)]_{11}[U(t_D, 0)]_{11} \times [S(\tau_1)]_{11}[V(\tau_1)]_{11}[V^\dagger(\tau_1)]_{12} \times [S^\dagger(\tau_1)]_{22}[U^\dagger(t_D, 0)]_{22}[V_p^\dagger(\tau_p)]_{23}[S_p^\dagger(\tau_p)]_{33}, \quad (2.22)$$

where we have assumed that $\rho(0) = |1\rangle\langle 1|$. Substituting Eqs. (2.8), (2.13), (2.17), and (2.19) into Eq. (2.22) yields a result of the form

$$\rho_{13}(\tau_1 + t_D + \tau_p) = \exp[-i(\omega_{AS}\tau_p - k_{AS}z)]\sigma_{13}(\tau_1, t_D), \quad (2.23a)$$

$$k_{AS} = k_L - k_S + k_{L2}. \quad (2.23b)$$

$\sigma_{13}(\tau_1, t_D)$ is independent of τ_p and z. From Eq. (2.4), the ensemble averaged polarization per molecule is given by

$$P^{NL} = \exp[-i(\omega_{AS}\tau_p - k_{AS}z)]\langle\mu_{13}\sigma_{13}(\tau_1, t_D)\rangle + \text{c.c.} \quad (2.24)$$

The anti-Stokes electric field obeys the equation,[21]

$$\nabla^2 E_{AS} - \frac{n^2}{c^2}\frac{\partial^2}{\partial t^2}E_{AS} = \frac{4\pi}{c^2}\frac{\partial^2}{\partial t^2}P^{NL}. \quad (2.25)$$

n is the refractive index of the sample, c is the speed of light and P^{NL} is the nonlinear polarization. The slowly varying amplitudes of the field and polarization are defined by

$$E_{AS}(z, t) = \tilde{E}_{AS}(z, t)\exp[i(k_{AS}z - \omega_{AS}t)] + \text{c.c.}, \quad (2.26a)$$

$$P^{NL}(z, t) = \tilde{P}(t)\exp[i(k_{AS}z - \omega_{AS}t)] + \text{c.c.} \quad (2.26b)$$

In the slowly varying amplitude approximation,[21] Eq. (2.25) reduces to

$$\frac{\partial}{\partial z}\tilde{E}_{AS} = \frac{2\pi\omega}{nc}\tilde{P}(t). \quad (2.27)$$

The field amplitude at the end of a sample of length l is therefore

$$\tilde{E}_{AS}(l, t) = \frac{2\pi\omega l}{nc}\tilde{P}(t). \quad (2.28)$$

The anti-Stokes RFID signal intensity is given by the absolute square of $\tilde{E}_{AS}(l, t)$ and is, therefore, proportional to the absolute square of $\tilde{P}(t)$, which can be obtained from Eq. (2.24):

$$\tilde{P}(t_D) = \langle\mu_{13}\sigma_{13}(\tau_1, t_D)\rangle. \quad (2.29)$$

The final result is

$$I_{RFID} = |\tilde{P}(t_D)|^2 = A_{RFID}|\chi_{RFID}(t_D)|^2, \quad (2.30a)$$

$$A_{RFID} = \lambda_{13}^2|\Omega_p|^2|\Omega_{13}|^2\Omega_{23}|^2(1/\gamma^4)\{(\Omega_3 - \omega_{AS})/[(\Omega_3 - \omega_{AS})^2 + 2|\Omega_p|^2]\}[(1/\gamma^4)(|\Omega_{13}|^2 - |\Omega_{23}|^2)^2(1 - \cos\theta_1)^2 + \sin^2\theta_1], \quad (2.30b)$$

$$\chi_{RFID}(t_D) = \left\langle \exp\left(i\int_0^{t_D} d\tau\, \Delta(\tau)\right)\right\rangle, \quad (2.30c)$$

$$\theta_1 = \omega\tau_1. \quad (2.30d)$$

The frequency ω in Eq. (2.30d) is defined in Eq. (2.13e). As pointed out by Hartmann,[17] ω is the frequency at which states $|1\rangle$ and $|2\rangle$ exchange population. θ_1, thus, plays the same role here as the pulse "area" in an optical experiment. In fact, if the Rabi frequencies $|\Omega_{13}|$ and $|\Omega_{23}|$ are set equal, the RFID intensity is proportional to $\sin^2\theta_1$, which is the pulse area dependence of the optical FID signal.[22] The t_D dependence of the signal is given by $\chi_{RFID}(t_D)$ in Eq. (2.30c), which is the Fourier transform of the ordinary line shape. Thus, the time dependence of the RFID signal has the same information content as the time dependence of the signal in an optical FID experiment. The time scale of the decay of the RFID signal is determined by the full linewidth. If the line is broadened by a combination of static (inhomogeneous) and dynamic (homogeneous) broadening, the RFID cannot be used to obtain dynamical information. This point will be discussed further in the following sections.

The macroscopic polarization, induced by the RB pulse sequence, can be calculated with an analogous procedure. The system is excited with a pair of pulses of the form of Eq. (2.1) for a time τ_1, evolves freely for t_D, is excited with a second pair of pulses for a time τ_2, evolves freely for t, and then is probed with a pulse of duration τ_p. The density matrix element ρ_{13} at the end of the probe pulse is the sum of a term proportional to $\rho_{12}(\tau_1 + t_D + \tau_2 + t)$ and a term proportional to $\rho_{13}(\tau_1 + t_D + \tau_2 + t)$. As in the RFID calculation, we assume that the excitation process is sufficiently nonresonant that we can neglect the coherence induced between levels $|1\rangle$ and $|3\rangle$ by the two pairs of excitation pulses. Therefore, we need only consider the term in ρ_{13} that is proportional to $\rho_{12}(\tau_1 + t_D + \tau_2 + t)$. $\rho_{13}(\tau_1 + t_D + \tau_2 + t + \tau_p)$ is the sum of a term that gives rise to the echo signal and terms that correspond to the RFID signal induced by the first and second pairs of excitation pulses. Here we wish to consider only the echo term. The echo term has different temporal and spatial characteristics from the RFID terms, which enables one to isolate it both in theory and in practice. For a system with inhomogeneous broadening, the echo signal is a maximum at $t = t_D$.[23] The RFID signal induced by the second pair of excitation pulses is a maximum at $t = 0$. Thus, the echo contribution to ρ_{13} can be obtained by selecting the terms in ρ_{13} that are maximized at $t = t_D$. The echo term in ρ_{13} can also be obtained by examining the spatial dependence of the various contributions to ρ_{13}. The RFID signal induced by the second pair of pulses has the wave vector $k_{L2} + k'_L - k'_S$, where k'_L is the

wave vector of the second pump pulse and k'_S is the wave vector of the second Stokes pulse. The echo signal has the wave vector $k_E = 2(k'_L - k'_S) - (k_L - k_S) + k_{L2}$. Using either of these criteria, we can unambiguously isolate the term in ρ_{13} that is associated with the echo. We denote this term ρ^E_{13}:

$$\begin{aligned}\rho^E_{13}(\tau_1 + t_D + \tau_2 + t + \tau_p) &= [S_p(\tau_p)]_{11}[V_p(\tau_p)]_{11}[U(t,0)]_{11}[S(\tau_2)]_{11}[V(\tau_2)]_{12} \\ &\times [U(t_D,0)]_{22}[S(\tau_1)]_{22}[V(\tau_1)]_{21}[V^\dagger(\tau_1)]_{11}[S^\dagger(\tau_1)]_{11} \\ &\times [U^\dagger(t_D,0)]_{11}[V^\dagger(\tau_2)]_{12}[S^\dagger(\tau_2)]_{22}[U^\dagger(t,0)]_{22} \\ &\times [V^\dagger_p(\tau_p)]_{23}[S^\dagger_p(\tau_p)]_{33}. \end{aligned} \tag{2.31}$$

This expression can be evaluated with the matrix elements given in Eqs. (2.5), (2.8), (2.13), (2.17), and (2.19). ρ^E_{13} has the form

$$\begin{aligned}\rho^E_{13}(\tau_1 + t_D + \tau_2 + t + \tau_p) &= \exp[i(k_E z - w_{AS}\tau_p)]\,\Sigma_{13}(\tau_1, t_D, \tau_2, t), \end{aligned} \tag{2.32a}$$

$$k_E = 2(k'_L - k'_S) - (k_L - k_S) + k_{L2}, \tag{2.32b}$$

where Σ_{13} does not depend on z or τ_p. In analogy with Eq. (2.29), the slowly varying part of the polarization is given by

$$\tilde{P}(t_D + t) = \langle \mu_{13}\Sigma_{13}(\tau_1, t_D, \tau_2, t)\rangle. \tag{2.33}$$

The signal intensity for an optically thin sample is given by the absolute square of Eq. (2.33):

$$I_{RE} = A_{RE}|\chi_{RE}(t, t_D)|^2, \tag{2.34a}$$

$$\begin{aligned}A_{RE} &= \mu^2_{13}|\Omega_p|^2|\Omega'_{13}|^4|\Omega'_{23}|^4|\Omega_{13}|^2|\Omega_{23}|^2 \\ &\times\left[\frac{\Omega_3 - \omega_{AS}}{(\Omega_3 - \omega_{AS})^2 + 2|\Omega_p|^2}\right]^2 \sin^4(\theta_2/2)(1/\gamma')^8(1/\gamma)^4 \\ &\times[(1/\gamma^4)(1-\cos\theta_1)^2(|\Omega_{13}|^2 - |\Omega_{23}|^2)^2 + \sin^2\theta_1], \end{aligned} \tag{2.34b}$$

$$\chi_{RE}(t, t_D) = \left\langle \exp\left[i\left(\int_{t_D}^{t+t_D} \Delta(\tau)d\tau - \int_0^{t_D} \Delta(\tau)d\tau \right)\right]\right\rangle. \tag{2.34c}$$

θ_2 is the area of the second pulse, given by

$$\theta_2 = \omega'\tau_2, \tag{2.35a}$$

$$\omega' = \frac{(\gamma')^2}{\Omega_3 - \omega_L}. \tag{2.35b}$$

If the Rabi frequencies $|\Omega_{13}|$ and $|\Omega_{23}|$ are equal, the RE intensity is proportional to $\sin^4(\theta_2/2)\sin^2(\theta_1)$, which is the well known pulse area dependence for the photon echo.[22] The time dependence of the RE signal is given by $\chi_{RE}(t, t_D)$ in Eq. (2.34c). This time dependence is identical to that of the photon echo.[23] Thus, the information content of the RE decay is equivalent to that of a photon echo, which can be used to extract homogeneous dephasing times from systems with inhomogeneously broadened lines. The time dependences of the RFID and RE signals are discussed in the following section.

III. RESULTS AND DISCUSSION

The distinction between the information content of the RFID signal [Eqs. (2.30)] and that of the RE signal [Eqs. (2.34)] can be emphasized by rewriting these expressions in terms of equilibrium correlation functions of the vibrational coordinate operator $\hat{q}(t)$, defined by

$$\hat{q}(t) = U^\dagger(t,0)\hat{q}U(t,0), \tag{3.1}$$

$$\hat{q} = |1\rangle\langle 2| + |2\rangle\langle 1|. \tag{3.2}$$

The propagator $U(t,0)$, which is defined in Eq. (2.5b), describes the time evolution of the system in the absence of external fields. In the Appendix, we show that $\chi_{RFID}(t_D)$ in Eq. (2.30c) can be written as a two $\hat{q}$, two time correlation function:

$$\chi_{RFID}(t_D) = \langle \mathrm{Tr}\,\hat{q}(t_D)\hat{q}(0)\rho(0)\rangle^*, \tag{3.3}$$

where the brackets denote an average over the fluctuating energy of state $|2\rangle$. $\rho(0)$ is the equilibrium density matrix of the system. In deriving Eq. (3.3), it was assumed that $\rho(0) = |1\rangle\langle 1|$. Comparison of Eqs. (1.1) and (3.3) yields

$$\chi_{RFID}(t_D) = [I_0(t_D)]^*. \tag{3.4}$$

Similarly χ_{RE} in Eq. (2.34c) can be written as a four $\hat{q}$, three-time correlation function (see the Appendix):

$$\chi_{RE}(t, t_D) = \langle \mathrm{Tr}\,\hat{q}(-t - t_D)\hat{q}(-t_D)\hat{q}(0)\hat{q}(-t_D)\rho(0)\rangle. \tag{3.5}$$

From the time translational invariance of equilibrium correlation functions, Eq. (3.5) can be written as

$$\chi_{RE}(t, t_D) = \langle \mathrm{Tr}\,\hat{q}(-t)\hat{q}(0)\hat{q}(t_D)\hat{q}(0)\rho(0)\rangle. \tag{3.6}$$

Equation (3.6) is a special case of an expression derived by Skinner, Andersen, and Fayer[24] for photon echoes from generalized two-level systems. Thus, the information content of the RFID observable, or any other observable that depends only on the correlation function $I_0(t)$, must be equivalent to that of a steady state line shape measurement. Only observables like the RE or photon echo, which depend on higher order correlation functions, have the possibility of providing dynamical information that cannot be obtained from the ordinary line shape [Eq. (1.2)].

Equations (3.3) and (3.6) were derived under the low temperature assumption $\rho(0) = |1\rangle\langle 1|$. In the Appendix, we also derive more general expressions for χ_{RFID} and χ_{RE} that are valid for arbitrary temperature. It is shown that within the rotating wave approximation, the relation between $I_0(\omega)$ and $\chi_{RFID}(t)$ is preserved.

The averages over the fluctuating energy of state $|2\rangle$ in Eqs. (3.3) and (3.6) can be carried out in a straightforward manner if $\Delta(t)$ is taken to be a Gaussian variable.[6–8] In this case, χ_{RFID} is given by

$$\chi_{RFID}(t_D) = \exp[-g(t_D)], \tag{3.7}$$

$$g(t) = \int_0^t d\tau_1 \int_0^{\tau_1} d\tau_2 \langle \Delta(\tau_1 - \tau_2)\Delta(0)\rangle, \tag{3.8}$$

and χ_{RE} is

$$\chi_{RE}(t, t_D) = \exp[-2g(t) - 2g(t_D) + g(t + t_D)]. \tag{3.9}$$

We first consider dephasing that is induced by two independent processes that modulate the energy of state $|2\rangle$:

$$\Delta(t) = \Delta_1(t) + \Delta_2(t), \tag{3.10a}$$

$$\langle \Delta(t)\Delta(0)\rangle = D_1^2 \exp(-\Lambda_1|t|) + D_2^2 \exp(-\Lambda_2|t|). \tag{3.10b}$$

D_n and Λ_n are, respectively, the magnitude and inverse time scale of process n. Substituting Eq. (3.10b) into Eq. (3.8) gives

$$g(t) = g_1(t) + g_2(t), \tag{3.11}$$

$$g_n(t) = (D_n/\Lambda_n)^2[\exp(-\Lambda_n t) - 1 + \Lambda_n t]. \tag{3.12}$$

Substitution of Eqs. (3.11) and (3.12) into Eqs. (3.7) and (3.9) will give general expressions for the RE and RFID observables for a system with two dephasing mechanisms of arbitrary time scale and magnitude.

For illustrative purposes, we take the Markovian or rapid modulation limit for process 1 ($\Lambda_1/D_1 \gg 1$), and the static limit for process 2 ($\Lambda_2/D_2 \ll 1$). Under these conditions, processes 1 and 2 correspond respectively to homogeneous and inhomogeneous line broadening. In this case we have

$$g_1(t) = \Gamma_1 t, \tag{3.13}$$

where

$$\Gamma_1 = D_1^2/\Lambda_1, \tag{3.14}$$

and

$$g_2(t) = (D_2 t)^2/2. \tag{3.15}$$

Substitution of Eqs. (3.13)–(3.15) into Eqs. (3.7), (3.9), and (3.11) yields

$$I_{\mathrm{RFID}}(t_D) \propto \exp[-2\Gamma_1 t_D]\exp[-D_2^2 t_D^2], \tag{3.16}$$

$$I_{\mathrm{RE}}(2t_D) \propto \exp[-4\Gamma_1 t_D]. \tag{3.17}$$

In Eq. (3.17), the delay time between excitation pulses has been set equal to the delay time between the second excitation and the probe ($t = t_D$). The decay of the RFID will be influenced by both processes, while the decay of the RE yields the homogeneous dephasing rate, Γ_1. When the rapid modulation limit is taken for both processes ($\Lambda_1/D_1 \gg 1$; $\Lambda_2/D_2 \gg 1$), the signals are given by

$$I_{\mathrm{RFID}}(t_D) \propto \exp[-2(\Gamma_1 + \Gamma_2)t_D], \tag{3.18}$$

$$I_{\mathrm{RE}}(2t_D) \propto \exp[-4(\Gamma_1 + \Gamma_2)t_D], \tag{3.19}$$

$$\Gamma_2 = D_2^2/\Lambda_2. \tag{3.20}$$

In this limit, the line is homogeneously broadened, and the information content of the two observables becomes identical.

Figure 3 shows logarithmic plots of the RE signal, calculated from Eqs. (3.9) and (3.12). All plots are calculated for $\Lambda_1 = 100$, $D_1 = D_2 = 10$. Plots A, B, and C are calculated respectively for $\Lambda_2 = 10^{-6}$, 10^2, 1. In all cases, process 1 causes homogeneous line broadening ($\Lambda_1/D_1 \gg 1$). In case A, $\Lambda_2/D_2 \ll 1$. In this case, the RE signal is nonexponential at very short times, but becomes exponential with decay constant $4\Gamma_1$, as predicted by Eq. (3.17). The deviation from exponential behavior at short times arises because the condition $\Lambda_1 t \gg 1$ that leads to Eq. (3.13) is not satisfied for sufficiently short times. In case B, process 2 has a time scale identical to that of process 1 ($\Gamma_1 = \Gamma_2$). In this case, the RE signal is nonexponential at very short times for the reason just given, but it becomes exponential with decay constant $4(\Gamma_1 + \Gamma_2) = 8\Gamma_1$, as predicted by Eq. (3.19). In case C, process 2 has a time scale that is comparable in magnitude to the time scale of observation. In this case, the RE signal is *nonexponential* on the time scale of observation. Figure 3 shows that if vibrational dephasing is caused by two different processes with arbitrary time scales, the observed RE signal is, in general, nonexponential. The signal will be exponential (except at very short times) in two limiting cases. The first such case holds when the two processes occur on very different time scales. In this case, one process is "dynamic" on the time scale of observation, and the other is "static", relative to this time scale. The line broadening in such a system has homogeneous and inhomogeneous components. The second limiting case that leads to an exponential RE signal occurs, when both processes are dynamic on the time scale of observation. Such a system has a homogeneously broadened line.

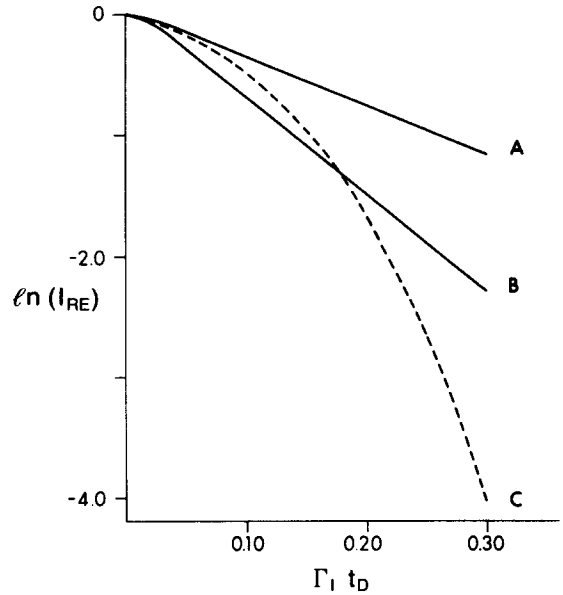

FIG. 3. Raman echo signal, calculated from Eqs. (3.9) and (3.12). $\Lambda_1 = 10^2$, $D_1 = D_2 = 10$. $\Gamma_1 = D_1^2/\Lambda_1$. (A) $\Lambda_2 = 10^{-6}$. (B) $\Lambda_2 = 10^2$. (C) $\Lambda_2 = 1$. Exponential RE signals will be observed from a system with two dephasing mechanisms if both processes are fast on the experimental time scale (B), or if one process is fast and the other is slow on this time scale (A). Otherwise, the decay will be nonexponential. (C).

We next consider another model, which was discussed briefly in Sec. I. In this model, the system is made up of M molecular species, and each species is taken to have a homogeneously broadened, spontaneous Raman line. The line shape for this system is given in Eq. (1.3). From Eqs. (1.3), (3.4), and (3.6), we have

$$\chi_{\mathrm{RFID}}(t_D) = \sum_j N_j \exp[i\omega_j t_D - \Gamma_j t_D], \tag{3.21}$$

$$\chi_{\mathrm{RE}}(t_D, t_D) = \sum_j N_j \exp[-2\Gamma_j t_D]. \tag{3.22}$$

Species j has relative concentration N_j and a line centered at ω_j with width $2\Gamma_j$. Equations (3.21) and (3.22) show that if all species have the same homogeneous linewidth ($\Gamma_j = \Gamma$ for all j), then this width can be determined unambiguously with the RE, but can only be obtained from the RFID if the lines are well separated. To illustrate this point, we consider a model system of three components with $N_1 = 0.2$,

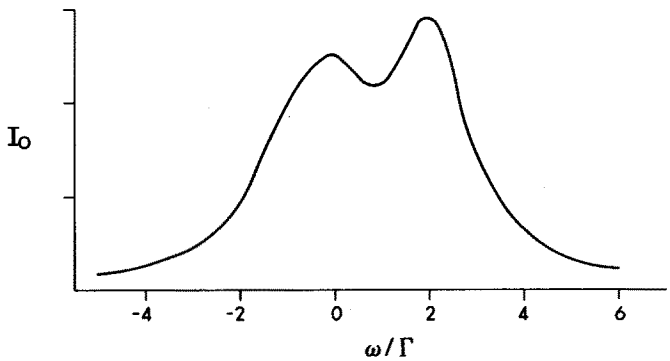

FIG. 4. Isotropic Raman line shape for a three-component system. Each component has relative concentration N_j, resonance frequency ω_j, and homogeneous dephasing rate Γ. $N_1 = 0.2$, $N_2 = 0.3$, $N_3 = 0.5$, $\omega_1 = -\Gamma$, $\omega_2 = 0$, $\omega_3 = 2\Gamma$. The RFID and RE signals from this system are shown in Fig. 5.

$N_2 = 0.3$, $N_3 = 0.5$, $(\omega_2 - \omega_1)/\Gamma = 1$, $(\omega_3 - \omega_2)/\Gamma = 2$. All components have homogeneous linewidths of 2Γ. The isotropic Raman line shape for this system is shown in Fig. 4. The lines overlap, and the line of species 1 cannot be resolved. Figure 5 shows logarithmic plots of the RFID and RE signals from this system. If the Raman lines of the three species were well separated, such a plot of the RFID signal would show a pattern of beats superimposed on a decay with slope 2Γ. However, for the case of Fig. 5, the period of the beats is long compared to experimental times and Γ cannot be determined from the observed RFID signal. Γ can be determined from the RE signal whose logarithmic plot is linear with slope 4Γ.

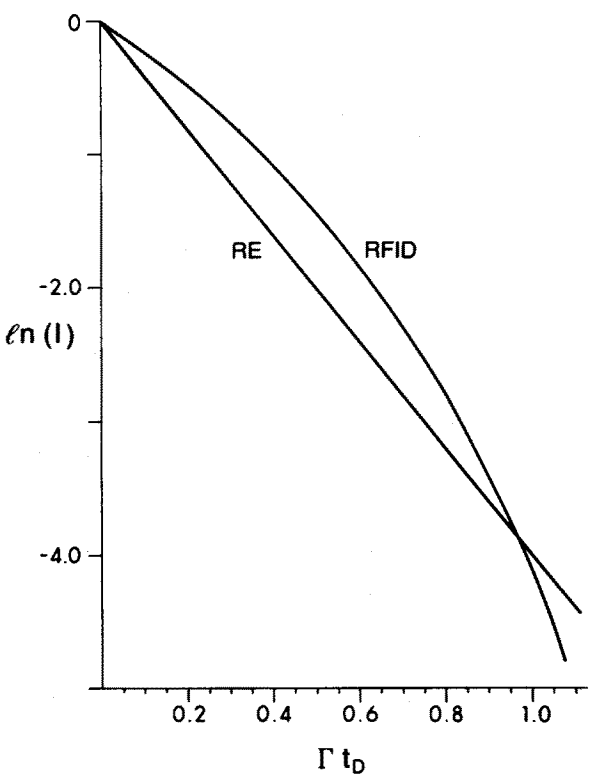

FIG. 5. Raman free induction decay and Raman echo signals from the three-component system, whose isotropic Raman line shape is shown in Fig. 4. Γ cannot be unambiguously determined from the RFID signal. The logarithmic plot of the RE signal for this system is linear with slope 4Γ.

IV. COMPARISON TO PREVIOUS WORK FOR OPTICALLY THIN SAMPLES

In Secs. II and III, we carried out a calculation of the RFID observable for an optically thin sample and short pulses and concluded that the information content of this observable is the same as that of the isotropic Raman line shape $[\hat{I}_0(\omega)]$. Previous theoretical treatments of the RFID have led to the opposite conclusion, namely that the RFID experiment, by virtue of the phase matching condition, is, in principle, capable of measuring homogeneous dephasing times in a system whose line shape is characterized by static inhomogeneous broadening. The first such treatment was carried out by Laubereau, Wochner, and Kaiser,[14(a)] who considered a model system composed of several distinct types of molecules, with each molecular type characterized by a different vibrational frequency [Eq. (1.3)]. Each vibration is modeled by an oscillator with a phenomenological damping. This model represents the system studied experimentally by these workers, in which the liquid is composed of molecules of differing isotopic composition and hence slightly different vibrational frequencies. The system studied was CCl_4, which is made up of $C^{35}Cl_4$, $C^{35}Cl_3^{37}Cl$, $C^{35}Cl_2^{37}Cl_2$, and $C^{37}Cl_4$. Their theoretical treatment was later generalized by Oxtoby.[5(c)] We will discuss the calculation as presented by Oxtoby.[5(a)] We reproduce below the equations from that work that relate to the generation of the anti-Stokes RFID signal:

$$E_{\rm AS} = \sum_j 1/2 E_{{\rm AS}j} \exp[i(k_{{\rm AS}j} z - \omega_{{\rm AS}j} t)] + \text{c.c.}, \quad (4.1)$$

$$\omega_{{\rm AS}j} = \omega_{L2} + \omega_j, \quad (4.2)$$

$$\left(\frac{\partial}{\partial z} + \frac{1}{v_{\rm AS}}\frac{\partial}{\partial t}\right) E_{{\rm AS}j} \propto -iN_j E_{L2}(t - t_D) Q_j \exp(i\Delta k_j z), \quad (4.3)$$

$$\Delta k_j = k_{L2} + k_L - k_{\rm S} - k_{{\rm AS}j}, \quad (4.4)$$

$$I_{\rm RFID}(t_D) \propto \left| \sum_j E_{{\rm AS}j}(l, t_D) \exp[i(k_{{\rm AS}j} l - \omega_{{\rm AS}j} t_D)] \right|^2, \quad (4.5)$$

$$I_{\rm RFID}(t_D) \propto \left| \sum_j N_j Q_j(l, t_D)[1 + (2\Delta k_j \Delta l)^2]^{-1/2} \times \exp[i(\Delta\omega_j t_D + \delta_j)] \right|^2 \quad (4.6)$$

$$\Delta\omega_j = \omega_L - \omega_{\rm S} - \omega_j, \quad (4.7)$$

$$Q_j(l, t_D) \propto \exp(-t_D/T_2), \quad (4.8)$$

$$\delta_j = -\arctan(2\Delta k_j \Delta l). \quad (4.9)$$

Subscripts AS, $L2$, L, and S refer respectively to the anti-Stokes signal, the probe pulse, the initial excitation pulse, and the initial Stokes pulse that accompanies the excitation. The subscript j labels the molecular type. Q_j is the slowly varying part of the coherent vibrational amplitude of species j. $v_{\rm AS}$ is the group velocity of the anti-Stokes signal. t_D is the delay time between the excitation pulses and the probe pulse. N_j is the fraction of molecules of type j. ω_j is the resonance vibrational frequency of the jth molecular type. l is the length of the sample, and Δl is the effective interaction length. Equation (4.6) was derived with the assumption that both

excitation and probe pulses are sufficiently short that dephasing can be neglected during the pulses. (This assumption was also made by us in Sec. II of this work.) If $\Delta k_j \Delta l \ll 1$ for all j, then Eq. (4.6) reduces to

$$I_{\mathrm{RFID}}(t_D) \propto \left| \sum_j N_j \exp(-t_D/T_2) \exp(i\Delta\omega_j t_D) \right|^2. \quad (4.10)$$

This is the square of the Fourier transform of the isotropic Raman line shape. However, if $\Delta k_j \Delta l \ll 1$ for $j = j'$, but $\Delta k_j \Delta l \gg 1$ for $j \neq j'$, Eq. (4.6) becomes

$$I_{\mathrm{RFID}}(t_D) \propto \exp(-2t_D/T_2). \quad (4.11)$$

Thus, Eq. (4.6) predicts that the RFID experiment is capable of selectively measuring the dephasing of the component labeled j'.

The crucial step in this derivation, which leads to the apparent selectivity, is the assumption that each molecular species j generates its own anti-Stokes field with frequency mismatch $\Delta\omega_j$ and a corresponding wave vector mismatch Δk_j [Eq. (4.1)]. This assumption is, of course, valid, when the spontaneous Raman line shape I_0 consists of a series of well-resolved lines whose spacing is much larger than T_2^{-1} (i.e., $\Delta\omega_j \gg T_2^{-1}$). In this case, however, the ordinary Raman line shape I_0 is already "selective," and the coherent Raman selectivity is uninteresting. The selectivity is of interest in the opposite limit when the lines do overlap ($\Delta\omega_j \lesssim T_2^{-1}$). In this case, however, we cannot tell the anti-Stokes field with which species to interact. *Equation (4.1), which assumes that E_{AS} is a sum of independent contributions from the various species is, therefore, wrong and is the source for the apparent selectivity.* The problem with Eq. (4.1) was recognized by Zinth *et al.*,[14(b)] who suggested that it may be corrected by modifying the time dependence of $E_{\mathrm{AS}j}$. We shall now show how the results of our Secs. II and III can be obtained from Eqs. (4.1)–(4.9), when this error is corrected. Instead of Eq. (4.1), we write

$$E_{\mathrm{AS}} = 1/2 \tilde{E}_{\mathrm{AS}} \exp[i(k_{\mathrm{AS}} z - \omega_{\mathrm{AS}} t)] + \text{c.c.}, \quad (4.12)$$

where k_{AS} and ω_{AS} are not associated with individual molecular species. This is equivalent to performing a general Fourier decomposition of the anti-Stokes field and considering the behavior of a particular component with frequency ω_{AS} and wave vector k_{AS}. The allowed values of k_{AS} and ω_{AS} will be determined from the resulting equations. Equation (4.3) is replaced by

$$\left(\frac{\partial}{\partial z} + \frac{1}{v_{\mathrm{AS}}}\frac{\partial}{\partial t}\right)\tilde{E}_{\mathrm{AS}} \propto -i \sum_j N_j E_{L2}(t - t_D) Q_j \exp(i\Delta k z) \times \exp[i(\omega_{\mathrm{AS}} - \omega_{L2} - \omega_j)t], \quad (4.13)$$

where

$$\Delta k = k_{L2} + k_L - k_{\mathrm{S}} - k_{\mathrm{AS}}. \quad (4.14)$$

Equation (4.6) is replaced by

$$I_{\mathrm{RFID}}(t_D) \propto \left| \frac{\exp(i\delta)}{[1 + (2\Delta k \Delta l)^2]^{1/2}} \sum_j N_j Q_j(l, t_D) \times \exp(i\Delta\omega_j t_D) \right|^2, \quad (4.15)$$

where δ is defined as in Eq. (4.9) with Δk_j of Eq. (4.4) replaced by Δk of Eq. (4.14). $I_{\mathrm{RFID}}(t_D)$ will have appreciable magnitude only if $\Delta k \Delta l \ll 1$. Therefore, if Δl is sufficiently large, we obtain the phase matching condition

$$k_{\mathrm{AS}} = k_{L2} + k_L - k_{\mathrm{S}}, \quad (4.16)$$

which is the same condition derived in Sec. II. [See Eq. (2.23b).] According to Eq. (4.15), the RFID signal is proportional to the absolute square of the Fourier transform of the isotropic Raman line shape, as in Eq. (4.10). This result is in agreement with our analysis in Sec. III, which leads to Eq. (3.21).

It is important to emphasize the difference between our conclusion concerning the absence of selectivity of the RFID experiment and that reached by Zinth, Polland, Laubereau, and Kaiser.[14(b)] In this work, the authors present new experimental data that indicate that their RFID measurements do not provide T_2 times for individual molecular types, as was earlier believed. Their theoretical analysis is similar to that of the earlier work by Laubereau, Wochner, and Kaiser[14(a)] and to that outlined by Oxtoby.[5(a)] They present a final expression for the signal that is similar to Eq. (4.6) but conclude that it is not possible in practice in the case of the CCl_4 system to achieve the phase matching condition that would lead to selectivity. Our statement is a stronger one. Equation (4.6) should be replaced with Eq. (4.15). For the experimental conditions of short pulses and an optically thin sample, the RFID signal contains the same dynamical information as does the isotropic Raman line shape. *The phase matching condition is irrelevant to the issue of selectivity for the RFID.*

Zinth, Nuss, and Kaiser[25] have shown that the RFID experiment can be used as a line-narrowing technique to resolve overlapping Raman lines. Consider an RFID experiment carried out on a system with a homogeneously broadened Raman line shape. The frequency spectrum of the signal is measured as a function of t_D, the delay time between excitation and probe pulses. We assume that the duration of the excitation process is small compared to T_2 but make no restriction on the duration of the probe pulse. Under these circumstances, the frequency-resolved signal $I(\Omega)$ is given by

$$I(\Omega) \propto \left| \int_0^\infty dt \exp(i\Omega t) E_p(t - t_D) I_0(t) \right|^2, \quad (4.17)$$

where $E_p(t - t_D)$ is the temporal profile of the probe pulse. Zinth *et al.*[25] have shown that if the line is homogeneous $\{I_0(t) \sim \exp[-t/T_2]\}$ and the probe pulse has a Gaussian temporal profile, whose duration is long compared to T_2, then for sufficiently long t_D, $I(\Omega)$ is a Gaussian, whose width is determined only by the duration of the long probe pulse. This result can be understood qualitatively as follows. The integral in Eq. (4.17) is the Fourier transform of the product of a decaying exponential and a Gaussian centered at t_D. At long times the exponential is relatively flat compared to a Gaussian, so for a wide enough Gaussian centered at large enough t_D, the product of the Gaussian and the exponential resembles a Gaussian. The Fourier transform of this product will be a Gaussian whose width is determined only by the duration of the probe pulse. Thus, if the probe pulse is sufficiently long, the observed linewidth can be narrower than the spontaneous linewidth $2T_2^{-1}$. Zinth *et al.* have used this technique to resolve the closely spaced Raman lines of hydrogen bonded aggregates of pyridine and methanol.[26] It must be emphasized that these results are completely consistent with our conclusions concerning the lack of selectivity

of the RFID experiment since the signal still depends on the weak field line shape $I_0(t)$. In the line-narrowing experiments, the observed linewidths are determined by laser pulse durations, not by intrinsic molecular processes. Thus, although the technique can be used to resolve the spectral peaks arising from different types of molecules in solution, it cannot provide information about relaxation processes affecting the individual molecular species that is not contained in a spontaneous Raman line shape.

V. OPTICALLY DENSE SAMPLES, PROPAGATION EFFECTS, AND THE HIGH LASER DEPLETION REGIME

The calculation of the RFID observable presented in Secs. II and III and the previous calculations discussed in Sec. IV were carried out under the assumption that the sample is optically thin. Harris and George have pointed out that in their RFID measurements the initial pump pulse can be significantly depleted, and that previous treatments are not directly applicable to the high laser depletion regime.[16] These workers have carried out numerical solutions of the Bloch–Maxwell equations for a system whose vibrational line shape is composed of several (three or five) components. They conclude that the RFID experiment achieves an enhanced selectivity for high laser depletion. They state that for sufficiently high laser depletion, the RFID experiment can be used to measure homogeneous dephasing times for systems with inhomogeneously broadened Raman lines. In this section, we discuss the distinction between depletion of the laser pulse and saturation of the vibrational transition. The treatment of George and Harris includes the former effect, but it neglects the latter. We show that under these assumptions the information content of the measurement is identical to that of the low-power line shape.

We reproduce below the Bloch–Maxwell equations for stimulated Raman scattering in an M component system, which were solved numerically by George and Harris[16]:

$$\frac{\partial e_L}{\partial z} = -g(\omega_L/2\omega_S)e_S \sum_{j=1}^{M} N_j q_j \exp(i\Delta\omega_j\tau), \tag{5.1}$$

$$\frac{\partial e_S}{\partial z} = (ge_L/2)\sum_{j=1}^{M} N_j q_j^* \exp(-i\Delta\omega_j\tau), \tag{5.2}$$

$$\left(\frac{\partial}{d\tau} + T_2^{-1}\right) q_j = (e_S^* e_L/T_2)\exp(-i\Delta\omega_j\tau). \tag{5.3}$$

e_S and e_L are scaled electric fields, given by $e = (\epsilon_0 c/2)^2 E$. q_j is the amplitude of the coherent vibration of the species labeled j. N_j is the fractional concentration of species j, and $\Delta\omega_j$ is defined in Eq. (4.7). g is the steady-state stimulated Raman gain constant. τ is the local time, which is related to the real time t by $\tau = t - zn/c$, where n is the refractive index. In general, the stimulated Raman process is described by *four* coupled equations which govern the time evolution of the following variables: the pump field, the Stokes field, the vibrational amplitude, and the population difference between the initial and final vibrational states.[27] Equations (5.1)–(5.3) do not include the equation of motion for the population difference. *Omission of this fourth equation, which is equivalent to neglecting saturation of the vibrational transition, is justified in the limit that all fields are weak.* Equation (5.1) describes the propagation of the pump field. If this field is not significantly depleted (i.e., if the sample is optically thin), then Eq. (5.1) can be neglected. The solution of the remaining pair of equations has been considered by several authors.[14(a),27] George and Harris include Eq. (5.1) in their calculation to account for depletion of the pump pulse but do not include a fourth equation for the population difference, which would have accounted for saturation of the transition. We demonstrate below that Eqs. (5.1)–(5.3) can be rewritten in a form in which the material response enters only as the low power line shape. This result holds, whether or not Eq. (5.1) is included. We demonstrate that in the weak field limit, in which Eqs. (5.1)–(5.3) are a valid description of the stimulated Raman process, the RFID experiment is not selective.

The microscopic information content of Eqs. (5.1)–(5.3) can be shown explicitly by formally solving Eq. (5.3) for q_j and substituting the result into the right sides of Eqs. (5.1) and (5.2). With the definition

$$\tilde{Q}_j = q_j \exp(i\Delta\omega_j\tau), \tag{5.4}$$

Eq. (5.3) can be written as

$$\left(\frac{\partial}{\partial\tau} - i\Delta\omega_j + T_2^{-1}\right)\tilde{Q}_j = e_S^* e_L/T_2. \tag{5.5}$$

Taking the Fourier transform of both sides of Eq. (5.5), yields

$$\hat{Q}_j(z,\omega) = [T_2^{-1} - i(\omega + \Delta\omega_j)]^{-1}\int_{-\infty}^{\infty} d\tau \times \exp(i\omega\tau)e_L(z,\tau)e_S^*(z,\tau), \tag{5.6}$$

where

$$\hat{Q}_j(z,\omega) = \int_{-\infty}^{\infty} d\tau \exp(i\omega\tau)\tilde{Q}_j(z,\tau). \tag{5.7}$$

$\tilde{Q}_j(z,\tau)$ can be obtained from Eq. (5.6) by applying the convolution theorem:

$$\tilde{Q}_j(z,\tau) = \int_{-\infty}^{\infty} d\tau_1 I_0^{(j)}(\tau-\tau_1)e_L(z,\tau_1)e_S^*(z,\tau_1). \tag{5.8}$$

$I_0^{(j)}(t)$ is the inverse Fourier transform of the homogeneous line shape of the species labeled j.

$$I_0^{(j)}(t) = \exp[i\Delta\omega_j t - |t|/T_2]. \tag{5.9}$$

Substitution of Eq. (5.8) into Eqs. (5.1) and (5.2) gives the following pair of integro-differential equations:

$$\frac{\partial}{\partial z}e_L(z,\tau) = -g(\omega_L/2\omega_S)e_S(z,\tau)\int_{-\infty}^{\tau} d\tau_1 \times I_0(\tau-\tau_1)e_L(z,\tau_1)e_S^*(z,\tau_1), \tag{5.10}$$

$$\frac{\partial}{\partial z}e_S(z,\tau) = [ge_L(z,\tau)/2]\int_{-\infty}^{\tau} d\tau_1 \times I_0^*(\tau-\tau_1)e_L^*(z,\tau_1)e_S(z,\tau_1). \tag{5.11}$$

The memory function $I_0(t)$ is the inverse Fourier transform of the isotropic, steady-state Raman line shape,

$$I_0(t) = \sum_{j=1}^{M} N_j I_0^{(j)}(t). \tag{5.12}$$

Equations (5.1)–(5.3) are, thus, equivalent to a pair of integral equations for the fields e_L and e_S, in which the inverse Fourier transform of the line shape is a memory kernel. It must be

emphasized that the material response enters in Eqs. (5.10) and (5.11) only through the total line shape $I_0(t)$ and not through the individual line shape functions of the various components, $I_0^{(j)}(t)$. This result is a consequence of the omission of the equation of motion for the population difference between the ground and excited vibrational states. If saturation of the transition is included, each component will behave differently under saturation, and the material response will depend on the individual $I_0^{(j)}(t)$ and not just on the total line shape $I_0(t)$.

Equations (5.1)–(5.3) describe the process by which a coherent vibrational excitation is created by stimulated Raman scattering. We next consider the remainder of the RFID experiment: free evolution and detection. Consider an experiment in which the system interacts with the fields e_L and e_S for a time t_p, evolves freely for a time t_D and then interacts with a short probe pulse. At time t_p, the coherent vibrational amplitude $\tilde{Q}_j$ is given by Eq. (5.8),

$$\tilde{Q}_j(z, \tau_p) = \int_0^{\tau_p} d\tau_1 \, I_0^{(j)}(\tau_p - \tau_1) e_L(z, \tau_1) e_S^*(z, \tau_1). \quad (5.13)$$

In Eq. (5.13), $\tau_p = t_p - zn/c$. The free evolution of $\tilde{Q}_j$ can be calculated from Eq. (5.5), with the fields set equal to zero:

$$\tilde{Q}_j(z, \tau_p + \tau_D) = I_0^{(j)}(\tau_D) \tilde{Q}_j(z, \tau_p). \quad (5.14)$$

From Eq. (5.9) we have

$$I_0^{(j)}(\tau_D) I_0^{(j)}(\tau_p - \tau_1) = I_0^{(j)}(\tau_D + \tau_p - \tau_1). \quad (5.15)$$

Substitution of Eq. (5.13) into Eq. (5.14) and application of Eq. (5.15), yields an expression for $\tilde{Q}_j$ at the time of probing:

$$\tilde{Q}_j(z, \tau_p + \tau_D) = \int_0^{\tau_p} d\tau_1 \, I_0^{(j)}(\tau_D + \tau_p - \tau_1) e_L(z, \tau_1) e_S^*(z, \tau_1). \quad (5.16)$$

The generation of a Stokes signal pulse from the interaction of the probe pulse with the vibrational coherence is described by Eq. (5.2), in which e_S should now be taken to represent the signal field and e_L the probe field. The right side of Eq. (5.2), is proportional to the complex conjugate of $\tilde{Q}$, which is defined by

$$\tilde{Q} = \sum_{j=1}^{M} N_j \tilde{Q}_j. \quad (5.17)$$

The value of $\tilde{Q}$ at the time of probing can be obtained from Eqs. (5.16) and (5.17):

$$\tilde{Q}(z, \tau_p + \tau_D) = \int_0^{\tau_p} d\tau_1 \, I_0(\tau_D + \tau_p - \tau_1) e_L(z, \tau_1) e_S^*(z, \tau_1). \quad (5.18)$$

$e_L(z,\tau)$ and $e_S(z, \tau)$ can be obtained from Eqs. (5.10) and (5.11), in which the material response enters only as $I_0(t)$, the total line shape. *Thus, the Stokes signal that is calculated from Eqs. (5.1)–(5.3) cannot contain information about the material that is not also present in the low power line shape function $I_0(t)$.*

The analysis of this section can be summarized as follows. Although Eqs. (5.1)–(5.3) include depletion of the pump laser pulse, they do not include saturation of the material transition. If material saturation is neglected, the calculated experimental observable depends on the material only through the low power line shape. Neglect of material saturation is justified in the limit that all fields are weak. *Thus, the RFID experiment is not selective for weak fields, whether or not the sample is optically dense.* If the laser pulses are long and strong (the large area regime), the RFID signal will no longer depend only on the low power line shape function. Since the saturation behavior of the ordinary line shape can be used to distinguish between homogeneous and inhomogeneous broadening (e.g., hole-burning spectroscopy), it is clear that the coherent transient experiment can also provide such information.

VI. SUMMARY AND CONCLUSIONS

In this work, we have considered the transient coherent Raman technique that has been developed by Kaiser, Laubereau, and co-workers[14,25,26] and Harris and co-workers[3] to study vibrational dephasing in liquids. We have addressed the question of the selectivity of this experiment, where selectivity is defined to be the capability to provide dynamical information that is not provided by an ordinary steady state line shape measurement.

In previous treatments of this problem, the calculation of the experimental observable is broken into three steps. In the first step, the Bloch–Maxwell equations are used to treat the propagation of the excitation and Stokes fields through the sample and to calculate the resulting polarization. In the second step, the time evolution of this polarization in the absence of radiation is determined. In the third step, the propagation of the probe and signal fields through the sample is treated. Our treatment in Secs. II and III shows that for optically thin samples and short laser pulses we can consider the entire process as one event and derive a correlation function expression for the observable. In contrast to previous work,[1,5,14(a)] the phase matching condition appears as a multiplicative factor and does not affect the selectivity of the experiment. We show that the information content of this observable is identical to that of an optical free induction decay experiment, and hence, that it is *not* selective. This finding is at variance with conclusions reached in previous theoretical treatments.[1,5,14(a)] In Sec. IV, we discuss the reason for the apparent selectivity predicted by these theories and show that it can be attributed to an incorrect analysis of the anti-Stokes signal field. These previous treatments are only valid in the limit in which the isotropic Raman line shape is composed of a series of well-resolved homogeneously broadened lines. In this case, homogeneous dephasing times can be determined using this technique, but the same information is present in the isotropic Raman line shape. In the case that the lines are not well resolved, that analysis breaks down. In Sec. IV, we show that analysis of Maxwell's equations yields the same result as the procedure of Secs. II and III.

Zinth, Nuss, and Kaiser have demonstrated both in theory[25] and in practice[26] that under certain conditions (discussed in Sec. IV) this technique can be used to resolve closely spaced Raman lines that are associated with different molecular species. This line narrowing is consistent with our conclusions, since the experimental linewidths are determined by laser pulse durations and not by intrinsic molecular relaxation processes.

The calculation of this observable by George and Harris[16] is discussed in Sec. V. They have argued that the experiment can be used to measure homogeneous dephasing times of a system with an inhomogeneously broadened Raman line shape, provided that the initial laser pump pulse is significantly depleted. In Sec. V, we make the distinction between laser pulse depletion, which occurs when the sample is optically dense, and saturation of the material transition, which occurs when the fields are strong. The Bloch–Maxwell equations considered by George and Harris include laser depletion, but they do not include material saturation. We demonstrate that the experimental observable calculated from these equations cannot show selectivity. If these equations are expanded to include material saturation, the information content of the experimental observable will no longer be identical to that of a low-power line shape measurement. There are, thus, two experimental conditions under which the experiment is not selective: short pulses of arbitrary strength and weak pulses of arbitrary duration. If the experiment is carried out with long, strong pulses, the signal will undoubtedly be characterized by some degree of selectivity. The signal, under these conditions, can be calculated numerically from the complete Bloch-Maxwell equations.

We have also considered the Raman echo experiment and have shown that this experiment can be used to go beyond the spontaneous Raman line shape in obtaining dynamical information. The theory of the Raman echo for a system with an inhomogeneously broadened line shape was originally developed by Hartmann.[17] Our present treatment generalizes that theory to an arbitrary time scale of the bath and is valid from the homogeneous to the inhomogeneous broadening limits. Raman echo experiments have been carried out in gases[18] and solids[19] but have not yet been applied to liquids. The Raman echo experiment has the capability of providing significant new information on the dynamics of vibrations in liquids.

ACKNOWLEDGMENTS

The support of the National Science Foundation, the Army Research Office, the Office of Naval Research, and the Petroleum Research Fund administered by the American Chemical Society is gratefully acknowledged. We wish to thank W. Kaiser and W. Zinth for most useful discussions.

APPENDIX

In this Appendix, we relate the RFID and RE signals to equilibrium correlation functions. We first assume that the molecule is initially in the ground vibronic state, $\rho(0)=|1\rangle\langle 1|$. We shall now prove Eq. (3.3), which relates the amplitude of the RFID signal to a two-time correlation function. $\chi_{\mathrm{RFID}}(t_D)$, defined in Eq. (2.30c), can be written as

$$\chi_{\mathrm{RFID}}(t_D)=\langle U_{11}^{\dagger}(-t_D,0)U_{22}(-t_D,0)\rangle, \tag{A1}$$

where $U(t_2,t_1)$ is the free propagator of Eq. (2.5). With the definition of the vibrational coordinate operator in Eq. (3.2), Eq. (A1) can be written as the equilibrium correlation function

$$\begin{aligned}\chi_{\mathrm{RFID}}(t_D)&=\langle \mathrm{Tr}\, U^{\dagger}(-t_D,0)\hat{q}U(-t_D,0)\hat{q}\rho(0)\rangle\\&=\langle \mathrm{Tr}\,\hat{q}(-t_D)\hat{q}(0)\rho(0)\rangle\\&=\langle \mathrm{Tr}\,\hat{q}(t_D)\hat{q}(0)\rho(0)\rangle^{*}.\end{aligned} \tag{A2}$$

In Eq. (A2), $\rho(0)$ is the equilibrium density matrix of the system, $\rho(0)=|1\rangle\langle 1|$. The angular brackets denote an average over the stochastic modulation of the energy of $|2\rangle$.

Equation (3.5), which relates the amplitude of the RE signal to a three-time correlation function, can be proved by the same procedure. $\chi_{\mathrm{RE}}(t,t_D)$ in Eq. (2.34c) can be expressed as

$$\begin{aligned}\chi_{\mathrm{RE}}(t,t_D)&=\langle U_{11}^{\dagger}(-t_D-t,-t_D)U_{22}(-t_D-t,-t_D)\\&\quad\times U_{22}^{\dagger}(-t_D,0)U_{11}(-t_D,0)\rangle\\&=\langle U_{11}^{\dagger}(-t_D-t,0)U_{22}(-t_D-t,0)U_{22}^{\dagger}(-t_D,0)\\&\quad\times U_{11}(-t_D,0)U_{22}^{\dagger}(-t_D,0)U_{11}(-t_D,0)\rangle.\end{aligned} \tag{A3}$$

Equation (A3) can be written in terms of $\hat{q}$ to yield Eq. (3.5):

$$\begin{aligned}&\chi_{\mathrm{RE}}(t,t_D)\\&\quad=\langle \mathrm{Tr}[\,U^{\dagger}(-t_D-t,0)\hat{q}U(-t_D-t,0)U^{\dagger}(-t_D,0)\\&\quad\times\hat{q}U(-t_D,0)\\&\qquad\times\hat{q}U^{\dagger}(-t_D,0)\hat{q}U(-t_D,0)\rho(0)]\rangle\\&\quad=\langle \mathrm{Tr}\,[\hat{q}(-t_D-t)\hat{q}(-t_D)\hat{q}(0)\hat{q}(-t_D)\rho(0)]\rangle.\end{aligned} \tag{A4}$$

We next relax the low temperature assumption that $\rho(0)=|1\rangle\langle 1|$, and consider the case $\rho(0)=\rho_{11}|1\rangle\langle 1|+\rho_{22}|2\rangle\langle 2|$, where $\rho_{22}\neq 0$. Equations (A1) and (A3) are still valid descriptions of the time dependence of the RFID and RE amplitudes for this case. However, Eqs. (A2) and (A4) should be replaced by

$$\chi_{\mathrm{RFID}}=\frac{\langle \mathrm{Tr}[\hat{A}^{\dagger}(t_D)\hat{A}(0)\rho(0)]\rangle^{*}}{\langle \mathrm{Tr}[\hat{A}^{\dagger}(0)\hat{A}(0)\rho(0)]\rangle^{*}}, \tag{A5}$$

$$\chi_{\mathrm{RE}}=\frac{\langle \mathrm{Tr}[\hat{A}^{\dagger}(-t)\hat{A}(0)\hat{A}^{\dagger}(t_D)\hat{A}(0)\rho(0)]\rangle}{\langle \mathrm{Tr}[\hat{A}^{\dagger}(0)\hat{A}(0)\hat{A}^{\dagger}(0)\hat{A}(0)\rho(0)]\rangle}, \tag{A6}$$

$$\hat{A}=|2\rangle\langle 1|, \tag{A7}$$

$$\hat{q}=\hat{A}^{\dagger}+\hat{A}. \tag{A8}$$

The correlation function in Eq. (A5) can still be related to the isotropic line shape function, $I_0(\omega)$:

$$I_0(\omega)=\int_{-\infty}^{\infty}dt\,\exp[i\omega t]\langle \mathrm{Tr}[\hat{q}(t)\hat{q}(0)\rho(0)]\rangle, \tag{A9}$$

$$\begin{aligned}\langle \mathrm{Tr}[\hat{q}(t)\hat{q}(0)\rho(0)]\rangle&=\langle \mathrm{Tr}[\hat{A}^{\dagger}(t)\hat{A}(0)\rho(0)]\rangle\\&\quad+\langle \mathrm{Tr}[\hat{A}(t)\hat{A}^{\dagger}(0)\rho(0)]\rangle.\end{aligned} \tag{A10}$$

Within the rotating wave approximation, only the first term on the right side of Eq. (A10) will contribute to the Fourier transform in Eq. (A9):

$$I_0(\omega)=\int_{-\infty}^{\infty}dt\,\exp[i\omega t]\langle \mathrm{Tr}[\hat{A}^{\dagger}(t)\hat{A}(0)\rho(0)]\rangle. \tag{A11}$$

Comparison of Eqs. (A5) and (A11) shows that the isotropic Raman line shape can be expressed as the Fourier transform of a correlation function whose absolute square gives the RFID time dependence, even at finite temperature.

[1]A. Laubereau and W. Kaiser, Rev. Mod. Phys. **50**, 607 (1978).
[2]J. Schroeder, V. H. Schiemann, and J. Jonas, Mol. Phys. **34**, 1501 (1977); J. Hyde Campbell, J. F. Fisher, and J. Jonas, J. Chem. Phys. **61**, 346 (1974).
[3]S. M. George, A. L. Harris, M. Berg, and C. B. Harris, J. Chem. Phys. **80**, 83 (1984); S. M. George, H. Auweter, and C. B. Harris, *ibid.* **73**, 5573 (1980); C. B. Harris, H. Auweter, and S. M. George, Phys. Rev. Lett. **44**, 737 (1980).
[4]S. F. Fischer and A. Laubereau, Chem. Phys. Lett. **35**, 6 (1975).
[5](a) D. W. Oxtoby, Adv. Chem. Phys. **40**, 1 (1979); (b) J. Phys. Chem. **87**, 3028 (1983); (c) J. Chem. Phys. **74**, 5371 (1981).
[6]D. Grimbert and S. Mukamel, J. Chem. Phys. **76**, 834 (1982).
[7]R. Kubo, in *Stochastic Processes in Chemical Physics*, edited by K. E. Shuler (Interscience, New York, 1969), p. 101.
[8]S. Mukamel, Phys. Rep. **93**, 1 (1982); Phys. Rev. A **26**, 617 (1982); **28**, 3480 (1983).
[9]R. W. Olson and M. D. Fayer, J. Phys. Chem. **84**, 2001 (1980).
[10]G. J. Small, in *Modern Problems in Condensed Matter Sciences*, edited by V. M. Agranovich and A. A. Maradudin (North Holland, Amsterdam, 1983); Vol. 4; R. W. Olson, H. W. H. Lee, F. G. Patterson, M. D. Fayer, R. M. Shelby, D. P. Burum, and R. M. MacFarlane, J. Chem. Phys. 77, 2283 (1982).
[11]J. Hegarty, W. M. Yen, and M. J. Weber, Phys. Rev. B **18**, 5816 (1978).
[12]R. L. Shoemaker, Annu. Rev. Phys. Chem. **30**, 239 (1979); W. H. Hesselink and D. A. Wiersma, in *Modern Problems in Condensed Matter Sciences*, edited by V. M. Agranovich and A. A. Maradudin (North Holland, Amsterdam, 1983), Vol. 4, p. 249.
[13](a) U. Haeberlen, *Advances in Magnetic Resonance* (Academic, New York, 1976), Suppl. 1; (b) W. S. Warren and A. H. Zewail, J. Chem. Phys. **78**, 2279 (1983).
[14](a) A. Laubereau, G. Wochner, and W. Kaiser, Phys. Rev. A **13**, 2212 (1976); (b) W. Zinth, H.-J. Polland, A. Laubereau, and W. Kaiser, Appl. Phys. B **26**, 77 (1981).
[15](a) S. Velsko, J. Trout, and R. M. Hochstrasser, J. Chem. Phys. **79**, 2114 (1983); (b) B. H. Hesp and D. A. Wiersma, Chem. Phys. Lett. **75**, 423 (1980); (c) C. L. Schosser and D. D. Dlott, J. Chem. Phys. **80**, 1394 (1984).
[16]S. George and C. B. Harris, Phys. Rev. A **28**, 863 (1983).
[17]S. R. Hartmann, IEEE J. Quantum Electron. **4**, 802 (1968).
[18]K. P. Leung, T. W. Mossberg, and S. R. Hartmann, Phys. Rev. A **25**, 3097 (1982).
[19]P. Hu, S. Geschwind, and T. M. Jedju, Phys. Rev. Lett. **37**, 1357 (1976).
[20]J. M. Ziman, *Elements of Advanced Quantum Theory* (Cambridge University, Cambridge, 1969), p. 63.
[21]Y. R. Shen, *The Principles of Nonlinear Optics* (Wiley, New York, 1984).
[22]L. Allen and J. H. Eberly, *Optical Resonance and Two-Level Atoms* (Wiley, New York, 1975).
[23]R. F. Loring and S. Mukamel, Chem. Phys. Lett. **114**, 426 (1985).
[24]J. L. Skinner, H. C. Andersen, and M. D. Fayer, Phys. Rev. A **24**, 1994 (1981).
[25]W. Zinth, M. C. Nuss, and W. Kaiser, Opt. Commun. **44**, 262 (1983).
[26]W. Zinth, M. C. Nuss, and W. Kaiser, Phys. Rev. A **30**, 1139 (1984).
[27]N. Bloembergen, Am. J. Phys. **35**, 989 (1967); R. L. Carman, F. Shimizu, C. S. Wang, and N. Bloembergen, Phys. Rev. A **2**, 60 (1970).